Synthesis of ZnS Nanowires and Assemblies by Carbothermal Chemical Vapor Deposition and Their Photoluminescence

Hua Zhang,[a] Shuyuan Zhang,*[a] Ming Zuo,[a] Gongpu Li,[a] and Jianguo Hou[a]

Keywords: Chemical vapor deposition / Luminescence / Nanostructures / Self-assembly / Zinc

A carbothermal method combined with CVD has been developed to synthesize ZnS nanowires and their self-assemblies at low temperatures. In this process, active carbon serves as reductant to react with sulfur, which then goes on to form ZnS nanowires. X-ray diffraction and X-ray photoelectron spectroscopy studies indicate that the samples are single-crystal wurtzite ZnS and are rich in sulfur. The nanowires have diameters ranging from 20 to 60 nm. High-resolution electron microscopy shows the [100] growth direction for the monodispersed nanowires and the different crystal orientation for the nanowires constituting the assembly. The photoluminescence (PL) peak is located at 490 nm. A vapor-solid (VS) mechanism might explain the formation of ZnS nanowires.

Introduction

Recently, there has been considerable interest in well-arranged nanostructures prepared by various methods, including template synthesis[1] and electrochemical deposition,[2] as they have potential applications in many areas, such as infrared photo detectors,[2] field emissions,[3] and as substrates for photocatalysis and photovoltaics.[4] As they are probably building blocks for well-ordered nanostructures and nanodevices,[5−7] one-dimensional nanomaterials have recently attracted much attention.[8−11] ZnS is an important II-VI semiconductor that possesses unique properties and has potential applications in numerous areas like optics,[12] electronics,[13] photocatalysis,[14] etc., and is especially promising in electric nanodevices. Except for our previously prepared ordered constructions[15] like flowers and sheets, only nanocombs[16] and microrods[17] composed of regularly arranged ZnS nanowires have been reported. ZnS nanowires and their assemblies have often been prepared by both solution methods[18] and thermal evaporation.[19] For the latter, ZnS powder precursors have generally been thermally evaporated under at 900−1600 °C. For example, ZnS-Si-ZnS triaxial nanowires[20] have been prepared by heating a mixture of SiO and ZnS powders to 1300 °C for 1 h and then to 1600 °C for 1.5 h. The obtained product was a composite material containing cubic Si and zincblende-structured ZnS. Wang's group[21] has employed a silicon wafer and Au films as substrate and catalyst, respectively. Wurtzite phase ZnS nanowires were successfully prepared by heating ZnS powders to 900 °C for 2 h,. According to Li and co-workers,[22] Zn/ZnS nanocables can be fabricated by thermal evaporation of ZnS and a graphite-powder mixture at 1300 °C for 5 h. In spite of these reports it is still a challenge to explore other new and versatile alternatives for the synthesis of pure ZnS nanowires and their assemblies at lower temperatures.

Here, we demonstrate that pure, wurtzite-phase ZnS nanowires can be prepared by a carbothermal, chemical-vapor-deposition method (CVD) by heating a mixture of activated carbon, sublimed sulfur and anhydrous $ZnCl_2$ powders to 500 °C. In addition, we have found that some self-assembled structures composed of ZnS nanowires coexist in the samples. Because of its lower temperature and versatility, this new fabrication method might present a new and easy way to form various kinds of sulfides. The green-blue emission of the as-grown ZnS nanowires and their assemblies may have potential applications in electronic/optical nanodevices.

Results and Discussion

The X-ray diffraction (XRD) pattern (see Supporting Information) of the as-prepared samples shows that the samples are well crystallized. All the peaks can be indexed as (100), (002), (101), (110), (103) and (112) crystal planes corresponding to JCPDS card 36-1450, which suggests that the samples are pure, wurtzite-phase, structured ZnS with lattice parameters $a = 3.820$ Å and $c = 6.257$ Å.

The Zn and S content in the ZnS nanowires was obtained from the X-ray photoelecton spectroscopy (XPS) patterns (Figure 1). No impurities, such as trace metals and other

[a] Structure Research Laboratory, University of Science and Technology of China
Hefei, Anhui 230026, People's Republic of China
Fax: + 86-0551-360-2803
E-mail: zhangsy@ustc.edu.cn

Supporting information for this article is available on the WWW under http://www.eurjic.org or from the author.

sulfides, are observed in the complete spectrum (see Supporting Information). The binding energy for Zn $2p^3$ (Figure 1a) is 1023.25 eV, which is a slight increase compared with that reported in the database[23] compiled and evaluated by Wagner, thus indicating a small difference in the chemical state of zinc in our samples. Curve 1 in Figure 1b shows the pattern of S $2p^3$ with two shoulders at about 162 and 164 eV. In order to determine the chemical states of sulfur, curves 2, 3 and 4, centered at 162.40, 163.40 and 164.60 eV, respectively, were fitted accompanied by their combined curve 5. Curves 2 and 3 represent the sulfur in ZnS; a small amount of elemental sulfur is responsible for curve 4. Therefore, the ratio of S to Zn in ZnS is about 1.077:1, which shows the richness of S instead of the sulfur deficiency generally found in previous papers.[24]

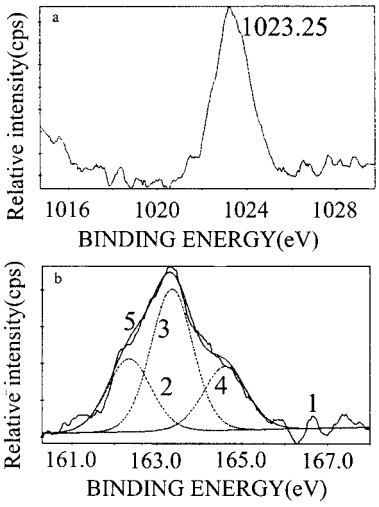

Figure 1. XPS patterns of the ZnS sample: (a) Zn $2p^3$ (b) S $2p^3$

Figure 2a displays a typical low-magnification transmission electron microscopy (TEM) image, which shows that the products consist of nanowires with uniform diameters ranging from 20 to 60 nm. The wires are long, straight and smooth with few other particles present. The electron diffraction (ED) pattern (inset) taken from a single nanowire (Figure 2b) can be indexed as the (100) and (001) planes of wurtzite-phase ZnS. Figure 2c shows a high-resolution electron microscopy (HREM) image, with a measured spacing of about 0.626 nm corresponding to the (001) plane. It can be clearly observed that the growth direction of the wire is perpendicular to [001], i.e. the [100] direction. The inset in the HREM image of another wire shows the two-dimensional lattice spacing, from which the (101) crystal plane, with a measured spacing of 0.293 nm, can clearly be seen.

Some regularly assembled structures, shown in Figures 3a and b, have been found in the as-prepared samples. From the high-magnification TEM image (Figure 3b) the characteristics of the wires can clearly be seen, especially from the different contrast and the places indicated by the arrows. These nanowires, with smooth surfaces and diameters in the range of 10−60 nm, are self-organized in the radial direction and are nearly parallel to each other, while in the thickness direction the self-organization can't be comfirmed from the contrast; this is different to the case of microrods,[17] where the assembly happens in two dimensions. The (001) and (002) crystal planes of the wurtzite phase can be identified in the ED pattern. The HREM image taken from the frame-labeled area is shown in Figure 3c. There are two different lattice spacings related to the two neighboring single nanowires. One is 0.313 nm, corresponding to the (002) plane, and the other is 0.227 nm, corresponding to the (102) plane. This indicates that not all the nanowires making up the assembly grow along the same crystal orientation.

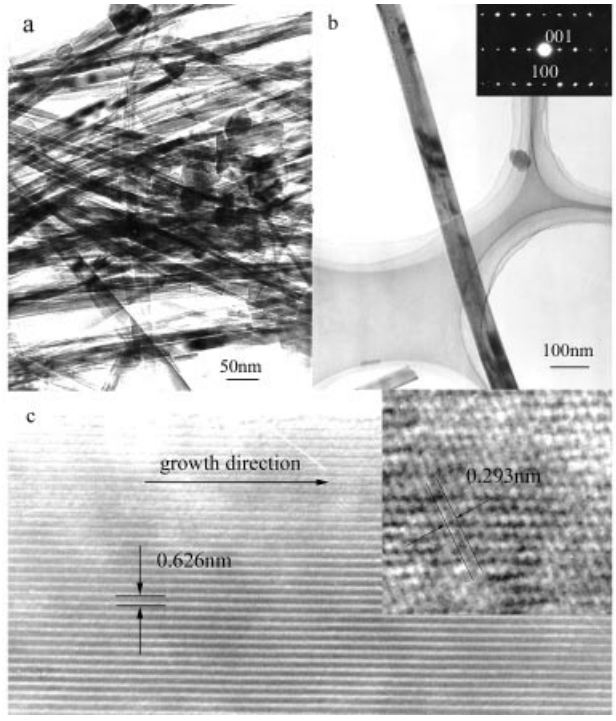

Figure 2. (a) TEM image of ZnS nanowires; (b) TEM image of a single ZnS nanowire and its ED pattern (inset); (c) one-dimensional and (inset) two-dimensional HREM images of a ZnS nanowire

The room-temperature photoluminescence (PL) spectrum of the as-synthesized ZnS nanowires and assemblies was measured with excitation and filter wavelengths of 313 nm and 350 nm, respectively. As shown in Figure 4, a strong emission peak is located at 490 nm, which is similar to that of the well-known ZnS-related luminescence (at about 480 nm) produced by zinc vacancies.[25] The ZnS nanomaterials reported previously have ultra-violet emission with bands in the range 400−450 nm[26−27] associated with the sulfur vacancy. It has been reported in previous work on ZnS that the vacancy states lie deeper in the gap than the interstitial states.[28] Therefore, in the case of the sulfur-rich nanowires containing no impurities reported here, we reasonably believe that the green-blue luminescence is attributed to zinc vacancies rather than the vacancy and interstitial sites of sulfur.

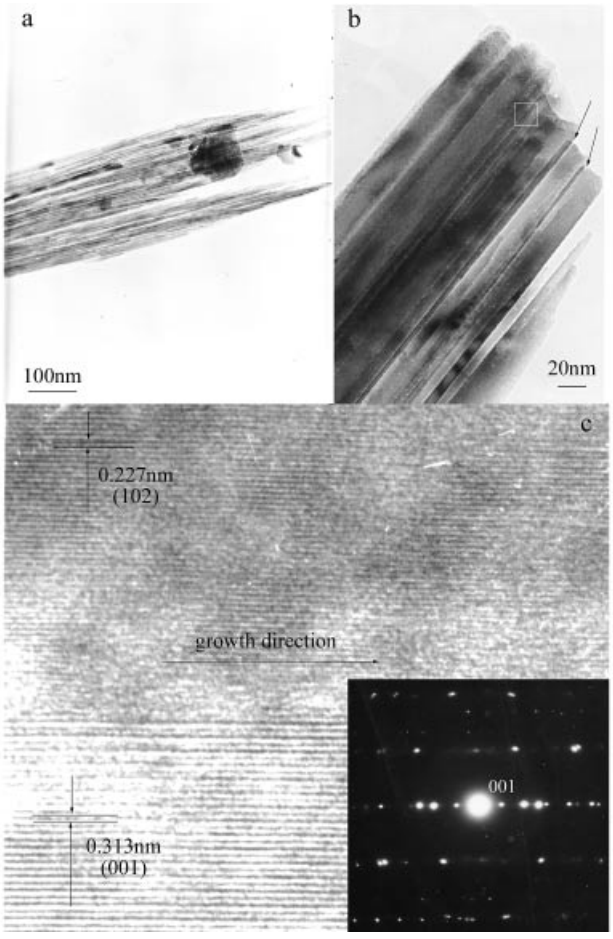

Figure 3. (a) and (b) TEM images of self-assembled ZnS nanowires and (inset) their ED pattern; (c) HREM image taken from the two, neighboring, frame-labeled single nanowires with two different lattice spacings: one is 0.313 nm corresponding to the (002) crystal plane, and the other is 0.227 nm corresponding to the (102) crystal plane: this indicates the different growth direction of the constituent nanowires

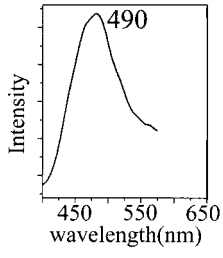

Figure 4. Room-temperature PL spectrum of the as-synthesized ZnS sample with excitation at 313 nm and a filter at 350 nm; the green-blue emission peak is located at 490 nm

To the best of our knowledge, the carbothermal reduction method is usually used to fabricate oxides,[29] carbides[30] and nitrides,[31] in which active carbon or graphite generally reacts with source chemicals containing O or N to generate intermediate compounds. It is well known that active carbon can serve as a reductant and react in a furnace with sulfur to generate CS_2, which can act as a sulfur source in the fabrication of sulfides.[32] Due to the low boiling point of CS_2 (b.p. 46.26 °C) and low melting point of $ZnCl_2$ (m.p. 318 °C),[33] there is enough vapor to react and the one-dimensional characteristic of CS_2 could contribute to the formation of ZnS nanowires. According to these ideas, we designed the above-described experiments and found that ZnS nanowires were synthesized successfully. In the absence of active carbon we only obtained nanoparticles. This synthesis method can be understood in terms of carbothermal CVD. The growth of one-dimensional nanomaterials by thermal evaporation is often explained by a vapor-liquid-solid (VLS)[34] or vapor-solid (VS)[35] growth mechanism. For example, the silicon nanowires reported by Yu[36] were synthesized on solid substrates by the VLS mechanism using Au or Zn nucleation catalysts. In this case, the presence of a big particle at the tip of the nanowire is commonly considered to be evidence for the operation of the VLS mechanism. Jiang's group has fabricated ZnS nanoribbons[37] by a VS mechanism through hydrogen-assisted thermal evaporation. Comparing the features of these two mechanisms, and with no tip-located particles present, the VS explanation may be operative in the formation process of our ZnS nanowires. The experimental conditions and the anisotropy might provide the external and internal driving forces for the crystal growth. Once the nucleation starts, the crystal grow in the preferential orientation of the ZnS crystal planes.

Conclusion

In summary, ZnS nanowires and their self-assemblies have been successfully prepared for the first time by a carbothermal CVD method at low temperature. The as-prepared samples are wurtzite-phase, single nanocrystals with uniform morphology. The mono-dispersed nanowires grow along the [100] direction and those nanowires constituting the self-assemblies grow in different crystal orientation. Possibly due to their sulfur-rich nature, the samples show strong green-blue emission at room temperature, which is consistent with the luminescence of the zinc vacancy. The growth of our ZnS nanowires can be explained by a VS mechanism. Because of its easy operation and versatility, this carbothermal CVD route may be extended to the synthesis of other kinds of sulfide semiconductor nanowires. Further improvements of the equipment and studies on the application of ZnS nanowires and their self-organized structures are in progress.

Experimental Section

All the employed reactants were commercial and analytical grade without any further purification. A thoroughly blended powder mixture of sublimed sulfur (S), active carbon (C), and anhydrous zinc chloride ($ZnCl_2$) with a molar ratio of 4:1:2 was put into a porcelain boat which was placed in the bottom of a short quartz tube (approx. 25 mm diameter and 10 cm length) closed at one end. The short tube was placed with the open end downstream in the

center of a long quartz tube (approx. 50 mm diameter and 1 m length) mounted in a horizontal furnace, which was sealed and high-purity nitrogen was passed through it for 2 h to purge the air from the system. After heating to 500 °C for 2 h, the tube furnace was allowed to cool to room temperature in a constant flow of nitrogen. White samples were collected from the inner wall of the short tube, and then washed with distilled water and absolute ethanol several times. The purity and phase structure of the products were obtained by X-ray powder diffraction (XRD) analysis, which was performed with a D/max-γA X-ray diffractometer (λ = 0.15405 nm). The composition of the samples was determined by XPS with an ESCALAB MKII electron spectrometer using Mg-K_α radiation as the source. The morphologies and microstructure were observed and analyzed by TEM and HREM with a JEOL-2010 transmission electron microscope using an acceleration voltage of 200 kV. The PL measurements were carried out with a HITACHI850-type visible-ultraviolet spectrophotometer with a 313 nm excitation and a 350 nm filter at room temperature. The XRD pattern and the complete XPS spectrum of our sample are available as Supporting Information.

Acknowledgments

This work was supported by the National Natural Science Foundation of China (grant no. 50132030).

[1] S. Han, X. Y. Shi, F. M. Zhou, *Nano Lett.* **2002**, *2*, 97−100.
[2] N. Kouklin, L. Menon, A. Z. Wong, D. W. Thompson, J. A. Woollam, P. F. Williams, S. Bandyopadhyay, *Appl. Phys. Lett.* **2001**, *79*, 4423−4425.
[3] J. Chen, S. Z. Deng, N. S. Xu, *Appl. Phys. Lett.* **2002**, *80*, 3620−3622.
[4] Y. Y. Wu, H. Q. Yan, P. D. Yang, *Top. Catal.* **2002**, *19*, 197−202.
[5] Y. Cui, C. M. Lieber, *Science* **2001**, *291*, 851−853.
[6] T. Rueckes, K. Kim, E. Joselerich, G. Y. Tseng, C. Cheung, C. M. Lieber, *Science* **2000**, *289*, 94−97.
[7] S. Noda, K. Tomoda, N. Yamamoto, A. Chutinan, *Science* **2000**, *289*, 604−606.
[8] S. M. Zhou, Y. S. Feng, L. D. Zhang, *Eur. J. Inorg. Chem.* **2003**, 1794−1797.
[9] X. D. Wang, P. X. Gao, J. Li, C. J. Summers, Z. L. Wang, *Adv. Mater.* **2002**, *14*, 1732−1735.
[10] J. W. Liu, M. W. Shao, Q. Tang, S. Y. Zhang, Y. T. Qian, *J. Phys. Chem. B* **2003**, *107*, 6329−6332.
[11] A. Govindaraj, F. L. Deepak, N. A. Gunari, C. N. R. Rao, *Isr. J. Chem.* **2001**, *41*, 23−30.
[12] L. V. Zavyalova, A. K. Savin, G. S. Svechnikov, *Displays* **1997**, *18*, 73−78.
[13] X. J. Liu, X. Cai, J. F. Mao, C. Y. Jin, *Appl. Surf. Sci.* **2001**, *183*, 103−110.
[14] H. Fujiwara, H. Hosokawa, K. Murakoshi, Y. Wada, S. Yanagida, *Langmuir* **1998**, *14*, 5154−5159.
[15] H. Zhang, S. Y. Zhang, D. Y. Pan, G. P. Li, S. Pan, J. G. Hou, *J. Nanosci. Nanotech.* **2004**, *4*, 209−213.
[16] C. Ma, D. Moore, J. Li, Z. L. Wang, *Adv. Mater.* **2003**, *15*, 228−231.
[17] Y. C. Zhu, Y. Bando, D. F. Xue, D. Golberg, *Adv. Mater.* **2004**, *16*, 831−834.
[18] Q. T. Zhao, L. S. Hou, R. Huang, *Chem. Commun.* **2003**, *6*, 971−972.
[19] Y. Jiang, X. M. Meng, J. Liu, Z. R. Hong, C. S. Lee, S. T. Lee, *Adv. Mater.* **2003**, *15*, 1195−1198.
[20] J. Q. Hu, Y. Bando, Z. W. Liu, T. Sekiguchi, D. Golberg, J. H. Zhan, *J. Am. Chem. Soc.* **2003**, *125*, 11306−11313.
[21] Y. W. Wang, L. D. Zhang, C. H. Liang, G. Z. Wang, X. S. Peng, *Chem. Phys. Lett.* **2002**, *357*, 314−316.
[22] Q. Li, C. R. Wang, *Appl. Phys. Lett.* **2003**, *82*, 1398−1400.
[23] C. D. Wagner, A. V. Naumkin, A. K. Vass, J. W. Allison, C. J. Powell, J. R. Rumble, Jr., *NIST X-ray Photoelectron Spectroscopy Database*, version 3.4, NIST Standard Reference Database 20 (web version).
[24] K. Manzoor, S. R. Vadera, N. Kumar, T. R. N. Kutty, *Mater. Chem. Phys.* **2003**, *82*, 718−725.
[25] S. Oda, H. Kukimoto, *J. Lumin.* **1979**, *18/19*, 829−835.
[26] J. F. Suyver, S. F. Wuister, J. J. Kelly, A. Meijerink, *Nano Lett.* **2001**, *1*, 429−433.
[27] W. G. Becker, A. J. Bard, *J. Phys. Chem.* **1983**, *87*, 4888−4893.
[28] D. Denzler, M. Olschewski, K. Sattler, *J. Appl. Phys.* **1998**, *84*, 2841−2845.
[29] H. T. Ng, B. Chen, J. Li, J. Han, M. Meyyappan, J. Wu, S. X. Li, E. E. Haller, *Appl. Phys. Lett.* **2003**, *82*, 2023−2025.
[30] J. A. Johnson, C. M. Hrenya, A. W. Weimer, *J. Am. Ceram. Soc.* **2002**, *85*, 2273−2280.
[31] H. Arik, *J. Eur. Ceram. Soc.* **2003**, *23*, 2005−2014.
[32] X. C. Jiang, Y. Xie, J. Lu, L. Y. Zhu, W. He, Y. T. Qian, *Chem. Mater.* **2001**, *13*, 1213−1218.
[33] J. A. Jean, *Lange's Handbook of Chemistry*, 13th ed., McGraw-Hill, New York, **1985**, p 4−34.
[34] C. Kawai, A. Yamakawa, *Ceram. Int.* **1998**, *24*, 135−138.
[35] Y. C. Zhu, Y. Bando, D. F. Xue, *Appl. Phys. Lett.* **2003**, *82*, 1769−1771.
[36] J. Y. Yu, S. W. Chung, J. R. Heath, *J. Phys. Chem. B* **2000**, *104*, 11864−11870.
[37] Y. Jiang, X. M. Meng, J. Liu, Z. Y. Xie, C. S. Lee, S. T. Lee, *Adv. Mater.* **2003**, *15*, 323−327.

Received August 1, 2004

